

1 **Genetic Markers and Predictive Factors Influencing the Aggressive**
2 **Behavior of Cerebral Cavernous Malformation**

3 Gustavo F. Galvão M.D, PhD, Luisa M. Trefilio, Andreza L. Salvio P.h.D, Elielson
4 V. da Silva M.S.c, Soniza V. Alves-Leon M.D, P.h.D, Fabrícia L. Fontes-Dantas
5 Pharm.D, P.h.D, Jorge M. de Souza M.D, PhD.

6

7 **ABSTRACT**

8 Biological behavior of Cerebral Cavernous Malformation (CCM) is still
9 controversial without clear-cut signature for biological mechanistic explanation of
10 lesion aggressiveness. There is plenty evidence implicating dysregulated
11 inflammatory and immune responses in vascular malformation pathogenesis,
12 including CCM. In the present study, we evaluated the predictive capacity of the
13 SNPs *VDR*^{rs7975232}, *VDR*^{rs731236}, *VDR*^{rs11568820} as well as expanded the analysis of
14 *PTPN2*^{rs72872125} and *FCGR2A*^{rs1801274} in relation to the aggressive behavior of
15 CCM and its implications in biological processes. This was a single-site
16 prospective observational cohort study with 103 patients enrolled, 42 had close
17 follow-up visits for a period of 4 years, focused on 2 main aspects of the disease:
18 (1) symptomatic event that composed both intracranial bleeding or epilepsy and
19 (2) precocity of symptoms. We report a novel observation that the *PTPN2*^{rs72872125}
20 CT and the *VDR*^{rs7975232} CC genotype were independently associated with an
21 asymptomatic phenotype. Additionally, *PTPN2*^{rs72872125} CC genotype and serum
22 level of GM-CSF could predict a diagnostic association with symptomatic
23 phenotype in CCM patients, while the *FCGR2A*^{rs1801274} GG genotype could
24 predict a symptomatic event during follow-up. The study also found a correlation
25 between *VDR*^{rs731236} AA and *VDR*^{rs11568820} CC genotype to the time to first
26 symptomatic event. In summary, this study provides valuable insights into the
27 genetic markers that could potentially impact the development and advancement
28 of CCM.

29

30 **KEYWORDS:** Cerebral Cavernous Malformation, Diagnostic Biomarker,
31 Prognostic Biomarker, *FCGR2A*, *PTPN2*, *VDR*

32

NOTE: This preprint reports new research that has not been certified by peer review and should not be used to guide clinical practice.

33

34

35 INTRODUCTION

36 Cerebral cavernous malformation (CCM) are vascular malformations
37 consisting of capillary-like channels with a single layer of endothelium and no
38 intervening nervous tissue^{1,2}. CCM are among the most common vascular
39 malformation of the central nervous system (CNS) affecting 0.5%–1% of the
40 population, with magnetic resonance image (MRI) as the gold standard for the
41 diagnosis and the lesions evaluation should include the hemosiderin-sensitive
42 techniques as the susceptibility-weighted imaging (SWI)^{3,4}. Intracerebral
43 hemorrhage (ICH) and seizure, are the main clinical manifestations, followed by
44 neurological disability without evidence of bleeding. However, many patients
45 remain asymptomatic throughout their life and it is not known what factors may
46 predict aggressive manifestations in individual cases^{4,5}.

47 Usually, single cavernomas are detected in patients affected by sporadic
48 forms and often associated with a developmental venous anomaly. Familial CCM
49 is mostly associated with the occurrence of multiple lesions that might increase
50 in number and size with aging⁶. The familial form of the disease is linked to
51 mutations on specific genes, (*CCM1/KRIT1*, *CCM2/MGC4607* and
52 *CCM3/PDCD10*), which encode distinct proteins involved in the endothelial cell
53 junction function and in the interaction with cytoskeletal proteins. The most
54 frequent and well-studied of the CCM genes is the *CCM1/KRIT1*, with mutational
55 analyses showing a Hispanic-American ancestral haplotype^{7,8}. CCMs are
56 characterized by an incomplete disease penetrance, being 80% to the CCM1
57 form, near 100% to the CCM2 and 60% to the CCM3 form^{9,10}. Furthermore, the
58 discovery of *PIK3CA* mutations in CCM lesions provides important new insights
59 into the genetic factors that contribute to the variable expression and progression
60 of the disease phenotype¹¹.

61 Biological behavior of CCM is still controversial without clear-cut signature
62 for biological mechanistic explanation of lesion aggressiveness. There is plenty
63 evidence implicating dysregulated inflammatory and immune responses in
64 vascular malformation pathogenesis, including CCM. Several dysregulated
65 pathways have been confirmed in the transcriptome of CCM lesions, which are
66 out of balance having an impact on the permeability of the blood-brain barrier and
67 the stability of endothelial tight junctions¹². Notably, inflammatory and immune

68 cells such as monocytes, macrophages, B and T cells, are present in human
69 CCM lesions as well as in mouse models of CCM^{13–17}. Recently, our group have
70 demonstrated an adaptive immune-cellular reaction to CCM within CD20+ and
71 CD68+ in the pericavernous tissue of an aggressive pharmaco-resistant epilepsy
72 patient¹⁸. Moreover, the severity of the disease has been linked to genetic
73 polymorphisms within inflammatory and immune response genes¹⁹.

74 The significance of certain genetic variants in the development of CCM has
75 been established, underscoring the need for further investigation into their
76 specific roles. Tang et al 2017 showed allele T for SNP in *TLR4* (rs10759930)
77 gene is associated with increased CCM lesion number²⁰. Some studies have
78 also identified genetic polymorphisms in genes related to oxidative stress with a
79 significant impact on inter-individual variability in CCM disease onset and severity
80²¹. Of particular interest, in a previous study, our group demonstrated the
81 association of *FCGR2A*^{rs1801274} GG and *PTPN2*^{rs72872125} CT genotype with a
82 symptomatic profile of CCM patients in a smaller cohort²².

83 In the present study, we evaluated the predictive capacity of the SNPs
84 *VDR*^{rs7975232}, *VDR*^{rs731236}, *VDR*^{rs11568820} as well as expanded the analysis of
85 *PTPN2*^{rs72872125} and *FCGR2A*^{rs1801274} in relation to the aggressive behavior of
86 CCM and its implications in biological processes. We also looked for plasmatic
87 inflammatory cytokines expressed in the patients, verifying a pattern of
88 heterogeneity of plasmatic expression and any correlation with the genetic
89 variation identified with different clinical phenotypes of CCM. Using a multi-step
90 Bayesian approach, we thought to build a biomarker that could predict a
91 diagnostic and a prognostic aggressive phenotype of CCM.

92

93 **METHODS**

94 ***Study Design and Population***

95 This was a single-site prospective observational cohort study. Qualified
96 researcher on human subjects conducted this study having been approved by
97 the National Council for Ethics in Research (CAAE 69409617.9.0000.5258).
98 Blood samples were collected between October 2017 to March 2023 and
99 informed consent was obtained. Strobe criteria were used to report the findings
100 of this study⁶³.

101 The epidemiological data were defined at each clinical assessment. Patients
102 were stratified as multiform when they harbor multiples CCM on SWI or Gecho
103 or as isolated form when they had a single lesion at the CNS. Both definitions
104 were based on MRI study with SWI or Gecho and the absence of venous
105 development anomalies in the multiple cases in proximity.

106 CCM clinical presentation were identified as symptomatic (hemorrhage or
107 seizure) and asymptomatic. Intracerebral hemorrhage was defined based on the
108 consensus of Cavernous Angiomas with Symptomatic Hemorrhage (CASH) ⁵⁰.

109 The solely epileptic patients were defined as not having achieved previous
110 hemorrhagic consensus and whom the MRI evaluation depicted no hint of
111 hemosiderin beyond the usual smooth and regular deposit around a CCM lesion.

112 In this study, we focused in 2 mains aspects of the disease: (1) symptomatic
113 event that composed both intracranial bleeding or epilepsy and (2) precocity of
114 symptoms. We considered that these presentations may reflect an aggressive
115 phenotype of the disease. We also designed six sub-group analysis in order to
116 check for correlation - 60 years or older, female, familiar form, pure epileptic
117 without signs of lesion bleeding, pure symptomatic bleeding and infratentorial
118 lesion. Among the 103 consecutive cases, 42 had closely follow-up visit for a
119 period of 4 years. The remaining patients either did not have a clinical follow-up
120 visit or underwent surgical resection.

121

122 ***Sample collection and processing***

123 Blood samples were collected with EDTA and processed by centrifugation at 720
124 × g and 4 °C for 5 min to separate the plasma. The plasma supernatants were
125 immediately stored at -80°C until further processing. The Genomic DNA (gDNA)
126 extraction was performed using the PureLink Genomic DNA Mini Kit according to
127 the manufacturer's recommendations (ThermoFisher Scientific, Waltham,
128 Massachusetts, USA). The quality of gDNA was determined by NanoDrop 2000
129 (ThermoFisher Scientific) followed by quantification using the Qubit dsDNA HS
130 Assay Kit (ThermoFisher Scientific) and Qubit Fluorometer3.0 (Thermo Fisher
131 Scientific).

132

133 ***Plasma isolation and Inflammatory Modulators Assessment***

134 Proinflammatory cytokine and chemokine levels in plasma were measured using
135 a multiparametric immunoassay based on XMap-labeled magnetic microbeads
136 (Luminex Corp – Austin, TX, USA). A human ProcartaPlex™ Panel (Invitrogen
137 – Waltham, MA, USA) was used to analyze a set of 18 cytokines and chemokines
138 (IL-1 β , IL-2, IL-4, IL-5, IL-6, IL-9, IL-10, IL-12p70, IL-13, IL-17A, IL-18, IL-21, IL-
139 22, IL-23, IL-27, GM-CSF and INF- γ). The samples were measured according to
140 the manufacturer's instructions and simultaneously to avoid potential batch, as
141 described previously, using a BioPlex MAGPIX system (Biorad -Hercules, CA,
142 USA)^{64,65}. Cyto/chemokine expression was measured in duplicate, and the levels
143 of inflammatory modulators were analyzed using Xponent v. 3.0 software
144 (Luminexcorp) and expressed in pg/ml.

145

146 ***Analysis of polymorphism of PTPN2^{rs72872125}, VDR^{rs7975232}, VDR^{rs731236},***
147 ***VDR^{rs11568820} and FCGR2A^{rs1801274} genes***

148 The SNPs investigated in this study are detailed in Table 1. The SNPs were
149 genotyped by allelic discrimination performed in QuantStudio™ 3 Real-Time PCR
150 System (ThermoFisher) using TaqMan SNP genotyping assays (ThermoFisher).
151 The characteristics of the *PTPN2^{rs72872125}*, *VDR^{rs7975232}*, *VDR^{rs731236}*, *VDR^{rs11568820}*
152 *and FCGR2A^{rs1801274}* genes were obtained from the SNP bank of the National
153 Center of Biotechnology Information - NCBI (<http://www.ncbi.nlm.nih.gov/>). The
154 probes for each SNP were produced by Applied Biosystems™ *rs72872125*
155 (C__98019281_10), *rs7975232* (C__28977635_10), *rs731236*
156 (C__2404008_10), *rs11568820* (C__2880808_10) and *rs1801274*
157 (9077561_20). As the assay was designed and standardized to work with the
158 same thermal cycles, a single protocol was applied for both genes. Briefly, PCR
159 was performed with a 25 μ L reaction mixture containing 10 ng DNA, TaqMan®
160 _Universal PCR Master Mix (1X), Probe TaqMan® _Gene Expression Assay
161 (1X), and DNase free water for the final volume. The Real Time PCR conditions
162 were: initially 60°C for 30 seconds and then 95°C for 10 min, and subsequently
163 40 cycles of amplification (95 °C for 15 seconds and 60°C for 1 min), and then
164 60°C for 30 seconds. The five selected SNPs were amplified on separate plates.

165

166 ***In silico Structural Prediction of FCGR2A^{rs1801274} Protein and Phylogenetic***
167 ***Analysis***

168 Since the *FCGR2A^{rs1801274}* SNP is the only with amino acid change, we performed
169 a structural analysis using bioinformatic tools. *FCGR2A^{rs1801274}* transcript
170 structure was predict by directly modifications of the wild-type *FCGR2A* using
171 FASTA sequence obtained on NCBI database ⁶⁶. The new FASTA file was
172 submitted to the Chimera software (developed by the Resource for Biocomputing,
173 Visualization, and Informatics at the University of California, San Francisco, with
174 support from NIH P41-GM103311) for overall structural analysis ⁶⁷.

175 The evolutionary history was inferred using the MEGA-X software using the
176 maximum likelihood method and Jones-Taylor-Thornton (JTT) matrix-based
177 model. We first gathered the *FCGR2A* wild-type sequence from Homo sapiens
178 and 19 other mammals to study the evolutionary conservation of this protein.
179 Structural alignment was performed using the muscle algorithm that allows
180 multiple sequencing alignment with high accuracy and high throughput ⁶⁸.

181

182 ***Statistical Analysis***

183 Statistical analyses were performed with STATA 13 (StataCorp LP, TX, USA) and
184 GraphPad Prism 9.0.0 MacOS (GraphPad Software, San Diego, California USA,
185 www.graphpad.com). Categorical variables were expressed as n (%) and
186 continuous data were given as mean and standard deviation (SD). A 2-tailed 2-
187 sample t test or Mann-Whitney test was applied for continuous variables while
188 the association between two categorical variables was measured by Pearson
189 Chi-square (χ^2) test when appropriate.

190 Allelic and genotypic frequencies were calculated for patient and control subjects
191 via direct gene counting. Genotypic distributions in Hardy–Weinberg equilibrium
192 (HWE) were evaluated by two-tailed χ^2 -test. Linkage disequilibrium (LD) were
193 analyzed using: Linkage Disequilibrium Calculator
194 (https://grch37.ensembl.org/Homo_sapiens/Tools/LD), LDlink on
195 <https://ldlink.nih.gov/> and Heatmap was plotted by
196 <https://www.bioinformatics.com.cn/en>. The degree of LD between SNPs is
197 represented by R^2 and D' .

198 Genetic polymorphisms were evaluated through a univariate and multivariable
199 binary logistic regression adjusting for sex, age and familiar form when adequate
200 in matter of phenotype (symptomatic and asymptomatic). Plasma cytokines were
201 also evaluated between genotypes and phenotypes (symptomatic and
202 asymptomatic). Values over 2 times de standard deviation were excluded from
203 analysis due to possible bias results.

204 Genetic polymorphism and plasma cytokines verified as statistically different
205 between groups (both diagnostic and prognostic) were combined through a
206 canonical discriminant function analysis in order to build a biomarker-model of
207 symptomatic profile. All the possible combinations showing significant
208 association in symptomatic individuals were build. Receiver Operating
209 Characteristic (ROC) curves were generated along with a computed area under
210 the curve (AUC) for each combination individually and ROC curves were
211 compared to identify if any of them were statically superior then the others. The
212 best model-biomarker to differentiate symptomatic and asymptomatic patients in
213 both diagnostic and prognostic scenario was selected according to the Akaike
214 Information Criteria (AIC), representing the best fit parsimonious model to the
215 data with the fewest number of predictors. The optimal cutoff point was generated
216 from ROC curves utilizing the Youden index method. Mann-Whitney test was
217 then used to verify the difference in values generated using the modeled equation
218 among symptomatic and asymptomatic patients and a logistic regression was
219 used to control for age and sex. A p value <0.05 was considered significant.

220 To balance baseline covariates between patients with and without symptoms
221 during follow-up we used a propensity score matching (PSM) strategy. The
222 strategy involved 1:1 pairing and nearest-neighbor methods. After PSM, the
223 distribution of gender, familial form, and age was balanced between the groups
224 and the biomarker analysis was remade.

225 Finally, A Kaplan-Meyer survivor analysis was carried out among patients who
226 presented different polymorphism combinations. Hazard ratios were calculated
227 with 95% confidence intervals through a log-rank test. Failure events were
228 determined according to if there had been symptomatic presentation at some
229 point in the patient's lifetime

230

231 Results

232 **Demographic and CCM lesions characteristics**

233 Out of 103 CCM patients enrolled in the study, 44 are multifocal/familial CCMs,
234 70 patients presented with symptomatic phenotype, which 48 presented a
235 symptomatic hemorrhage secondary to their CCM, and 22 presented with
236 seizures and no history or signs of CCM bleeding on MRI. The median age of
237 enrolment was 45.6, within a mean age of 41.6 in the symptomatic group and
238 53.7 in epileptic sub-group. There were no significant differences in terms of sex,
239 age and form (sporadic vs familial/multifocal) between the outcome groups
240 (Table 2).

241

242 **Association of $PTPN2^{rs72872125}$ and $VDR^{rs7975232}$ to a Symptomatic Phenotype** 243 **and Plasmatic Cytokine Levels**

244 The distribution of the genotypic frequencies of the $PTPN2^{rs72872125}$,
245 $VDR^{rs7975232}$, $VDR^{rs731236}$, $VDR^{rs11568820}$ and $FCGR2A^{rs1801274}$ in symptomatic and
246 asymptomatic patients are shown in Table 3. All genotypic distributions were in
247 Hardy-Weinberg equilibrium. Haplotype analysis indicated linkage disequilibrium
248 between $VDR^{rs7975232}$ and $VDR^{rs731236}$ ($D' > 0.99$), corroborating what has already
249 been found in other populations (Figure 1A and Supplementary material). While
250 the other combinations segregate independently $VDR^{rs11568820}$ and $VDR^{rs731236}$
251 ($D' > 0.04$), $VDR^{rs11568820}$ and $VDR^{rs7975232}$ ($D' > 0.317$) (Figure 1A and
252 Supplementary material). A higher frequency of the $PTPN2^{rs72872125}$ CT genotype
253 (OR 0.34, 95% CI 0.11-0.99, $p = 0.04$) and the $VDR^{rs7975232}$ CC genotype (OR
254 0.06, 95% CI 0.006-0.612, $p = 0.017$) was observed in asymptomatic phenotype
255 in the age, familiar and female adjusted multivariable analysis, when compared
256 with symptomatic patients (Table 3). The ROC analysis (Figure 1B) revealed that
257 patients with $PTPN2^{rs72872125}$ CT genotype had a modest Area Under de Curve
258 (AUC 0.420, SE 0.05 CI 95% 0.334-0.506) and $VDR^{rs7975232}$ CC individuals
259 (Figure 1C) had a poor accuracy (AUC 0.439, SE 0.03 CI 95% 0.370-0.508).

260 We also hypothesized that these genetic variants might influence the
261 plasmatic inflammation signature of the CCM patients. We found that patients
262 who harbor the $PTPN2^{rs72872125}$ CT genotype showed a higher plasma level of IL-
263 10 ($p = 0.0146$) (Figure 1D) and low levels of IL-18 ($p = 0.0450$) (Figure 1E) and

264 IFN- γ ($p = 0.0310$) (Figure 1F), while individuals with *VDR*^{rs7975232} at least one C
265 allele had low plasma levels of IL-27 ($p = 0.0055$) and IL-23 ($p = 0.0034$) (Figure
266 1G-H). For other SNPs no significant difference in the levels of immune markers
267 was observed. We did not observe any significant differences in the levels of
268 these plasma molecules in relation to patient sex and form (sporadic/solitary or
269 familial/multifocal).

270

271 **Performance of Diagnostic Biomarker**

272 In order to build a diagnostic biomarker of CCM activity that could improve
273 our previously published weighted biomarker formula, we tested new
274 combinations of genetic and cytokines factors. First, the previously published
275 diagnostic weighted biomarker was again confirmed to distinguish symptomatic
276 and asymptomatic patients with 14.2% sensitivity and 97.4% specificity (AUC
277 0.641 SE 0.06 CI 95% 0.512 – 0.770, $p = 0.03$), worse than the range reported
278 previously. A similar canonical discriminant analysis approach was then
279 implemented to determine if a weighted combination of different SNPs and
280 cytokines could improve the diagnostic association with symptomatic phenotype.
281 The best weighted-biomarker included the *PTPN2*^{rs72872125} CC genotype and
282 GMCSF plasma levels as formulated $-0,89*(GMCSF)+0,41*(PTPN2^{rs72872125}CC)$
283 (AUC 0.663, SE 0.06 CI 95% 0.534 – 0.792, $p = 0.01$) with a specificity and
284 sensitivity 85.7% and 41.3%, respectively (Figure 2A). This formula outperformed
285 all the other possible formula (Table 1 Supplement) that had a statistically
286 significant value. The median weighted combination value was 2.65-times
287 increased ($p = 0.01$) in symptomatic patients (median estimated value -0.36)
288 compared with asymptomatic individuals (median estimated value -0.97) (Figure
289 2B). The formula performed fairly in the sub-group analysis of hemorrhagic
290 patients (AUC 0.661, SE 0.07, CI 95% 0.517 – 0.806) but had a good accuracy
291 in familiar form of the disease (AUC 0.774, SE 0.09, CI 95% 0.595 – 0.953, $p =$
292 0.01) and patients with infratentorial lesions (AUC 0.804, SE 0.08, CI 95% 0.642
293 – 0.966, $p = 0.001$) (Figure 2 C-D). Female symptomatic patients, pure epileptic
294 patients and elderly patients were not statically significant.

295

296 ***Validation Cohort with Symptomatic Event during Follow-up: Building a***
297 ***Prognostic Biomarker***

298 We then tested if the newly weighted-diagnostic biomarker could act as a
299 prognostic biomarker in a sub-group analysis of 42 patients that were
300 prospectively followed-up after initial blood collection. 4 patients experienced a
301 symptomatic event (1 lesion growth, 2 symptomatic hemorrhage and 1 newly
302 onset epilepsy without signs of bleeding) while the others 38 stayed
303 asymptomatic during the next 4 years. The weighted-biomarker had a fair
304 accuracy (AUC 0.644, SE 0.078, CI 95% 0.491-0.976) in distinguishing these
305 patients (Figure 3A). In order to verify if other combination of genetic variants and
306 cytokines could act as a prognostic biomarker, we first tested the 5 SNPs in the
307 sub-group of 42 patients that were closely followed-up. We found an independent
308 statistically significant association of the *FCGR2A*^{rs1801274} GG genotype (OR
309 16.10, 95% CI 1.32 – 195.52, p = 0.029) in the age and familiar adjusted
310 multivariable analysis. This variant had an excellent accuracy (AUC 0.796, SE
311 0.12, CI 95% 0.631-0.897) in distinguishing these individuals (Figure 3B). We
312 further tested the same gene in a propensity matched subgroup. The presence
313 of the *FCGR2A*^{rs1801274} GG genotype could predict a symptomatic event with high
314 accuracy (AUC 0.875, SE 0.12, CI 95% 0.473-0.996) (Figure 3C). We also tested
315 if this mutation would maintain its accuracy power when comparing symptomatic
316 patients during follow-up and individuals who have never experienced any
317 symptoms. We also found that *FCGR2A*^{rs1801274} GG genotype could predict a
318 symptomatic event with high accuracy (AUC 0.829, SE 0.14, CI 95% 0.519 -
319 0.956) (Figure 3D).

320

321 ***In Silico Structural Analysis of Transcript FCGR2A^{rs1801274}***

322 *In silico* structural analysis prediction reveals that the *FCGR2A*^{rs1801274} leads to a
323 substitution of a histidine for an arginine at position 131 (Figure 3E). The
324 structural alignment predicts that the variation c.500A>G (p.His131Arg) occurred
325 in domain that appears to be conserved mainly in higher primates, within 30% of
326 the species sharing this site (Figure 3F).

327

328 ***VDR variants relates to Precocity of symptoms***

329 We tested if any of the *VDR* genetic variants could relate to a precocity of
330 symptoms in the CCM cohort. Patients with the *VDR*^{rs731236} AA genotype tend to
331 present their symptoms late in their life compared to those who did not have (HR
332 0.52, SE 0.14, CI 95% 0.299-0.909 $p = 0.020$) (Figure 4A). Also, individuals that
333 harbor the *VDR*^{rs11568820} CC genotype tend to have symptoms earlier (HR 1.58,
334 SE 0.46, CI 95% 1.092-2.282 $p = 0.016$ (Figure 3B).

335

336 Discussion

337 Neuroinflammation is increasingly a focus of research in symptomatic events in
338 CCM patients²³. In the present study, we evaluated a large and phenotypically
339 well characterized CCM cohort and provided some key information about the
340 genetic influence on the behavior of this unique neurovascular disease. Here, we
341 have found an individual higher frequency of *PTPN2*^{rs72872125} CT and the
342 *VDR*^{rs7975232} CC genotypes in asymptomatic patients, associated with changes in
343 cytokine levels, suggesting a possible protective role. Our main new observation
344 is that the combination of a balanced formula using the *PTPN2*^{rs72872125} CC
345 genotype and serum level of GM-CSF could predict a diagnostic association with
346 symptomatic phenotype in CCM patients, while the *FCGR2A*^{rs1801274} GG
347 genotype showed the best accuracy in predicting a symptomatic event in the next
348 years, possibly functioning as prognostic genetic biomarker. In previous studies,
349 we reported the association of this same variants with an aggressive phenotype
350 of cerebral cavernous malformation but in a smaller sample²². Furthermore,
351 another exciting discovery is that individuals with the *VDR*^{rs731236} AA and
352 *VDR*^{rs11568820} CC genotypes may experience an earlier onset of symptoms in the
353 CCM cohort.

354 To date, there have been few published studies on SNPs in the *PTPN2*
355 gene, and among them, a weak association with certain diseases or different
356 outcomes was found. However, it is important to highlight that in combination with
357 other variants they have been shown to possibly increase the susceptibility of
358 chronic inflammatory disorders, including rheumatoid arthritis, type 1 diabetes
359 and celiac disease^{24–28}. Furthermore, there have been research findings
360 indicating the presence of epistasis between *PTPN2* and *VDR* gene^{29,30}.
361 Interestingly, patients who inherit the *PTPN2*^{rs72872125} CT genotype have high

362 levels of IL-10 when compared with CC genotype (Figure 1). IL-10 is an anti-
363 inflammatory molecule, with a well-established function in restraining and
364 regulating both acute and chronic inflammatory processes^{31,32}. Lyne et al. (2019)
365 demonstrated that IL-10 is an important molecule present in diagnostic CASH
366 biomarker and the levels were decreased in cases of individuals who had
367 experienced symptomatic CCM hemorrhage in the prior year³³. Furthermore, the
368 CT genotype was associated with low levels of IL-18 and INF- γ (Figure 1), which
369 are increased in patients with epilepsy and CCM hemorrhagic phenotype^{34–36}.
370 The Canonical values derived from the best weighted formula combination with
371 GM-CSF were 2,65X higher in patients who suffered a subsequent symptomatic
372 event (Figure 2). Like this, the a weighted combination of *PTPN2*^{rs72872125} SNP
373 and GM-CSF levels is a potential diagnostic genetic biomarker for the
374 symptomatic phenotype in CCM patients.

375 We had also provided more evidence that the *FCGR2A*^{rs1801274} GG
376 genotype could act as a prognostic biomarker of the disease. The *FCGR2A* gene
377 is located on chromosome 1q23 and consists of seven exons, encoding a
378 member of a family of Fc γ receptors for immunoglobulin G (IgG). Through it is
379 expression in immune system cells such as macrophages, dendritic cells and
380 neutrophils, it is possible to link cellular and humoral immunity^{37,38}. The *FCGR2A*
381 rs1801274 variant leads to a substitution of a histidine (A allele) for an arginine
382 (G allele) at position 131, also known as H131R. This polymorphism is capable
383 to increase the binding affinity of FCGR2A to IgG, resulting in activation of the
384 FCGR2A signaling pathway and upregulation of IgG2-dependent phagocytosis
385^{39,40}. The GG genotype has been associated with several autoimmune diseases,
386 such as Systemic Lupus Erythematosus, Type 1 Diabetes Mellitus, Crohn's
387 Disease and others, based on its relationship with the release and stimulation of
388 responsive inflammatory processes⁴¹. Protein structure prediction using
389 bioinformatic tools is an important approach to understand the *FCGR2A* variants.
390 In this study we also performed an *in-silico* analysis that demonstrated that the
391 H131R position is strongly conserved among higher primates, which may be
392 related to its clinical importance.

393 Lyne et al 2019 showed an upregulation of *FCGR2B* gene in CASH
394 transcriptomic, shedding light on the importance of Fc γ receptors in CCM disease

395 ³³. FcγRII receptors mediates the C-reactive protein (CRP)-induced changes in
396 endothelial function and inflammatory response ^{42,43}. A higher binding avidity of
397 CRP to FcγRIIa on immune cells was identified for allotype FcγRIIa-R131
398 compared to other genotypes ⁴⁴. The variant homozygous genotype (GG) was
399 able to increase the expression of ICAM-1 and E-selectin in HUVEC (Human
400 Umbilical Vein Endothelial Cells) and the levels of tPA, MCP-1, and IL-6 secreted
401 ⁴⁵. In addition, the G allele resulted in a significant defect in endothelium
402 dependent vasodilatation and reduced NO activity during endothelial cell
403 stimulation in patients with hypercholesterolaemia, corroborating with what has
404 already been found in models of CCM ^{46,47}. This data could potentially impact our
405 comprehension of the pathophysiology of CCM disease as well as consequences
406 with regard to the interpretation of prognostic biomarker for follow-up of patients.

407 Growing evidence suggests that vitamin D signaling role in cavernous
408 malformation behavior ⁴⁸. Peripheral plasma vitamin D has been shown to reflect
409 the severity of CCM disease ^{49,50}. Indeed, cholecalciferol (vitamin D3), was shown
410 to decrease CCM lesion burden in a murine model of CCM, and to inhibit ROCK
411 activity, known to affect CCM development^{22,47}. The effects of vitamin D on the
412 immune system are accomplished by binding to the nuclear Vitamin D Receptor
413 (VDR). Some single nucleotide polymorphisms (SNPs) in genes involved in
414 vitamin D singling were reported to have association with vitamin D deficiency ⁵¹.
415 The *VDR*^{rs731236} also known as TaqI, is a synonymous variant, while *VDR*^{rs7975232}
416 (ApaI) and *VDR*^{rs11568820} are located in the 3' and 5'-untranslated regions of the
417 gene respectively. These SNPs do not alter the amino acid sequence in the VDR
418 protein, but they can exert influence on mRNA stability and gene transcription ⁵².
419 Especially in relation to *VDR*^{rs7975232}, the literature does not make clear its role in
420 relation to vitamin D levels, on the other hand we showed that patients who
421 carried the CC genotype have decreased levels of proinflammatory cytokines
422 (Figure 1). Corroborating with a possible protective role of the *VDR*^{rs7975232}CC
423 genotype, Jiang et al (2015) showed that A allele slightly increased the risk of
424 temporal lobe epilepsy in children ⁵³.

425 Age at the first symptom is also a fundamental information during the
426 counselling of CCM patients. Distinguishing individuals with higher chances of
427 precocity of symptoms that could influence their productive life is of great

428 importance to the CCM community. Our study provided the correlation between
429 *VDR*^{rs731236} AA and *VDR*^{rs11568820} CC genotypes to the time to first symptomatic
430 event (Figure 4). However, we could not demonstrate a straight correlation
431 between the *VDR*^{rs11568820} CC and *VDR*^{rs731236} AA genotype presence and the
432 blood concentration of any of the analyzed cytokines. The relationship between
433 VDR polymorphisms and susceptibility to autoimmunity diseases have been
434 conducted in different settings, while the results obtained so far are conflicting^{54–}
435 ⁵⁶. We hypothesized that VDR polymorphism may affect the way proinflammatory
436 cells react to the CCM in an autoimmunity fashion leading to molecular level
437 disruption. To the best of our knowledge, this is the first study to investigate the
438 associations between *VDR* polymorphisms and cerebral cavernous
439 malformations.

440 Previously reports demonstrated that CCM1/KRIT1 regulates vascular
441 permeability through interaction with CCM2/MGC4607 to stabilize endothelial
442 cell–cell junctions, and together they suppress RhoA activity and, thus, activation
443 of the RhoA effector ROCK⁵⁷. Mutation on these genes lead to augment of actin
444 stress fiber formation and increased permeability of CCMs^{58–60}. Moreli et al
445 (2007) have shown that BXL-628, a VDR agonist, prevented RhoA activation and
446 inhibits RhoA/Rho Kinase signaling in rat and human bladder⁶¹. Since vitamin D
447 is a natural agonist of VDR and animal models have suggested that fasudil and
448 high doses of atorvastatin promotes significant inhibition of CCM lesional
449 development and hemorrhage through the RhoA/Rho Kinase rational, it is
450 reasonable to suppose that the prognostic ability of low levels of serum vitamin
451 D is related to these VD/VDR interactions and its genetic variants.

452 Our study pioneers a novel classification denoted as the "aggressive
453 behavior" paradigm within cerebral cavernous malformations (CCM),
454 incorporating both hemorrhage and epilepsy as integral components of its
455 symptomatic criteria. This redefined paradigm marks a transformative departure,
456 acknowledging the critical role of epilepsy alongside hemorrhage in defining the
457 clinical spectrum of CCM. Unlike a diagnostic biomarker, which detects the
458 presence of a specific medical condition, a prognostic biomarker assesses the
459 likelihood of progression or stability of medical conditions ⁶². These biomarkers
460 contribute to a more precise and expedited diagnosis, as well as improved patient

461 follow-up. In summary, our study provides new pieces of evidence for possible
462 genetic biomarkers that may influence the behavior of cerebral cavernous
463 malformations. We report a novel observation that the *PTPN2*^{rs72872125} CT and
464 the *VDR*^{rs7975232} CC genotypes were independently associated with an
465 asymptomatic phenotype. Additionally, *PTPN2*^{rs72872125} CC genotype and serum
466 level of GM-CSF could predict a diagnostic association with symptomatic
467 phenotype in CCM patients, while the *FCGR2A*^{rs1801274} GG genotype could
468 predict a symptomatic event during follow-up. The study also found a correlation
469 between *VDR*^{rs731236} AA and *VDR*^{rs11568820} CC genotype to the time to first
470 symptomatic event. Overall, this study provided valuable information on the
471 genetic factors that may influence the development and progression of CCM.
472 Moreover, beyond the conventional genetic biomarker purview, our investigation
473 postulates a novel etiological framework. We posit an inflammatory cascade
474 precipitating a self-non-self-interaction, instigating an autoimmune response
475 against CCM. This theoretical construct delineates the changes of CCM from a
476 benign anatomical variant—traditionally construed as a common disease—into
477 an aggressive lesion, now occupying the realm of a rare affliction—the
478 aggressive behavior of CCM. This theoretical construct challenges extant
479 paradigms, accentuating the potential role of immune-mediated mechanisms in
480 the clinical trajectory of CCM, thereby offering prospects for targeted
481 immunomodulatory interventions. In essence, this study augments our
482 comprehension of genetic determinants influencing the advancement of CCM
483 while advancing a transformative hypothesis concerning the disease's underlying
484 inflammatory dynamics. These insights herald a paradigm shift in conceptualizing
485 the clinical spectrum of CCM, fostering an enriched landscape for future
486 investigative pursuits and potential therapeutic interventions aimed at modulating
487 the intricate inflammatory cascades underpinning the aggressive behavior of
488 CCM.

489

490 **Supplemental material**

491 Table Supplementary 1 (S1)

492

493 **Correspondence**

494 Fabrícia Lima Fontes-Dantas: ORCID <https://orcid.org/0000-0002-5201-0927>, e-
495 mail fabricia.fontesdantas@uerj.br;

496 Jorge Marcondes de Souza: ORCID <https://orcid.org/0000-0003-2412-8239>, e-
497 mail jormarcondes@gmail.com.

498

499 **Affiliations**

500 Laboratório de Neurociências Translacional, Programa de Pós-Graduação em
501 Neurologia, Universidade Federal do Estado do Rio de Janeiro, Rio de Janeiro,
502 Brasil (G.F.G., A.L.S., E.V.S., S.V.A.L.). Departamento de Neurocirurgia,
503 Hospital Universitário Clementino Fraga Filho, Universidade Federal do Rio de
504 Janeiro, Rio de Janeiro RJ, Brasil (G.F.G., J.M.S.). Departamento de
505 Farmacologia e Psicobiologia, Instituto de Biologia Roberto Alcântara Gomes,
506 Universidade Estadual do Rio de Janeiro, Rio de Janeiro, Brasil (L.M.T, F.L.F.D).
507 Instituto Biomédico, Universidade Federal do Estado do Rio de Janeiro, Rio de
508 Janeiro, Brasil (L.M.T). Departamento de Neurologia, Hospital Universitário
509 Clementino Fraga Filho, Universidade Federal do Rio de Janeiro, Rio de Janeiro,
510 Brasil (S.V.A.L.).

511

512 **Acknowledgements**

513 The authors thank the Cavernoma Alliance Brazil Research Institute – Aliança
514 Cavernoma Brasil for the logistic assistance.

515

516 **Sources of Funding**

517 The author(s) disclosed receipt of the following financial support for the research,
518 authorship, and/or publication of this article: Brazilian National Council for
519 Scientific and Technological Development (CNPq Number 440779/2016-2),
520 Senator Romario Faria parliamentary amendment (no. 37990007 EIND), financial
521 support of Coordination for the Improvement of Higher Education Personnel
522 (CAPES Number 88887.130752/2016-00), FAPERJ E-26/210.657/2021, E-
523 26/210.273/2018 and E-26/201.040/2021 and Chamada Pública
524 MCTI/FINEP/CT-INFRA-PROINFRA 02/2014 – Equipamentos Multiusuários –
525 Ref. nº 0097/2016. Thanks to Fundação de Amparo à Pesquisa do Estado do
526 Rio de Janeiro (FAPERJ) and Casa Hunter for the financial help to this Project.

527

528 **Disclosures**

529 The authors declare no competing interests

530

531 **References**

- 532 1. Flemming KD, Graff-Radford J, Aakre J, Kantarci K, Lanzino G, Brown
533 RDJ, Mielke MM, Roberts RO, Kremers W, Knopman DS, et al.
534 Population-Based Prevalence of Cerebral Cavernous Malformations in
535 Older Adults: Mayo Clinic Study of Aging. *JAMA Neurol.* 2017;74:801–
536 805.
- 537 2. Spiegler S, Rath M, Paperlein C, Felbor U. Cerebral Cavernous
538 Malformations: An Update on Prevalence, Molecular Genetic Analyses,
539 and Genetic Counselling. *Mol. Syndromol.* 2018;9:60–69.
- 540 3. de Souza JM, Domingues RC, Cruz LCH, Domingues FS, Iasbeck T,
541 Gasparetto EL. Susceptibility-Weighted Imaging for the Evaluation of
542 Patients with Familial Cerebral Cavernous Malformations: A Comparison
543 with T2-Weighted Fast Spin-Echo and Gradient-Echo Sequences. *Am. J.*
544 *Neuroradiol.* [Internet]. 2008;29:154–158. Available from:
545 <http://www.ajnr.org/lookup/doi/10.3174/ajnr.A0748>
- 546 4. Salman RA-S, Hall JM, Horne MA, Moultrie F, Josephson CB,
547 Bhattacharya JJ, Counsell CE, Murray GD, Papanastassiou V, Ritchie V,
548 et al. Untreated clinical course of cerebral cavernous malformations: a
549 prospective, population-based cohort study. *Lancet Neurol.* [Internet].
550 2012;11:217–224. Available from: [http://dx.doi.org/10.1016/S1474-](http://dx.doi.org/10.1016/S1474-4422(12)70004-2)
551 [4422\(12\)70004-2](http://dx.doi.org/10.1016/S1474-4422(12)70004-2)
- 552 5. Ironside JW. Pathology of tumours of the nervous system. (5th ed.). D. S.
553 Russell and L. J. Rubinstein. Edward Arnold, London, 1989. No. of pages:
554 1012. Price: £110.00. ISBN: 07131 4549 8. *J. Pathol.* [Internet].
555 1989;158:359–359. Available from:
556 <https://doi.org/10.1002/path.1711580413>
- 557 6. Weinsheimer S, Nelson J, Abla AA, Ko NU, Tsang C, Okoye O,
558 Zabramski JM, Akers A, Zafar A, Mabray MC, et al. Intracranial
559 Hemorrhage Rate and Lesion Burden in Patients With Familial Cerebral
560 Cavernous Malformation. *J. Am. Heart Assoc.* [Internet].
561 2023;12:e027572. Available from:
562 <https://www.ahajournals.org/doi/10.1161/JAHA.122.027572>
- 563 7. Dashti SR, Hoffer A, Hu YC, Selman WR. Molecular genetics of familial
564 cerebral cavernous malformations. *Neurosurg. Focus.* 2006;21:e2.
- 565 8. Gross BA, Lin N, Du R, Day AL. The natural history of intracranial
566 cavernous malformations. *Neurosurg. Focus.* 2011;30:E24.
- 567 9. Labauge P, Denier C, Bergametti F, Tournier-Lasserre E. Genetics of
568 cavernous angiomas. *Lancet Neurol.* [Internet]. 2007;6:237–244.
569 Available from:
570 <https://linkinghub.elsevier.com/retrieve/pii/S1474442207700534>

- 571 10. Gault J, Sain S, Hu L-J, Awad IA. SPECTRUM OF GENOTYPE AND
572 CLINICAL MANIFESTATIONS IN CEREBRAL CAVERNOUS
573 MALFORMATIONS. *Neurosurgery* [Internet]. 2006;59:1278–1285.
574 Available from: <https://journals.lww.com/00006123-200612000-00015>
- 575 11. Snellings DA, Hong CC, Ren AA, Lopez-Ramirez MA, Girard R, Srinath
576 A, Marchuk DA, Ginsberg MH, Awad IA, Kahn ML. Cerebral Cavernous
577 Malformation: From Mechanism to Therapy. *Circ. Res.* [Internet].
578 2021;129:195–215. Available from:
579 <https://www.ahajournals.org/doi/10.1161/CIRCRESAHA.121.318174>
- 580 12. Koskimäki J, Polster SP, Li Y, Romanos S, Srinath A, Zhang D, Carrión-
581 Penagos J, Lightle R, Moore T, Lyne SB, et al. Common transcriptome,
582 plasma molecules, and imaging signatures in the aging brain and a
583 Mendelian neurovascular disease, cerebral cavernous malformation.
584 *GeroScience* [Internet]. 2020;42:1351–1363. Available from:
585 <https://link.springer.com/10.1007/s11357-020-00201-4>
- 586 13. Shenkar R, Shi C, Check IJ, Lipton HL, Awad IA. Concepts and
587 hypotheses: inflammatory hypothesis in the pathogenesis of cerebral
588 cavernous malformations. *Neurosurgery*. 2007;61:693.
- 589 14. Shi C, Shenkar R, Du H, Duckworth E, Raja H, Batjer HH, Awad IA.
590 Immune response in human cerebral cavernous malformations. *Stroke*.
591 2009;40:1659–1665.
- 592 15. Shi C, Shenkar R, Kinloch A, Henderson SG, Shaaya M, Chong AS, Clark
593 MR, Awad IA. Immune complex formation and in situ B-cell clonal
594 expansion in human cerebral cavernous malformations. *J.*
595 *Neuroimmunol.* 2014;272:67–75.
- 596 16. Plummer NW, Gallione CJ, Srinivasan S, Zawistowski JS, Louis DN,
597 Marchuk DA. Loss of p53 sensitizes mice with a mutation in *Ccm1*
598 (*KRIT1*) to development of cerebral vascular malformations. *Am. J.*
599 *Pathol.* 2004;165:1509–1518.
- 600 17. Maddaluno L, Rudini N, Cuttano R, Bravi L, Giampietro C, Corada M,
601 Ferrarini L, Orsenigo F, Papa E, Boulday G, et al. EndMT contributes to
602 the onset and progression of cerebral cavernous malformations. *Nature*.
603 2013;498:492–496.
- 604 18. Fontes-Dantas FL, da Fontoura Galvão G, Veloso da Silva E, Alves-Leon
605 S, Cecília da Silva Rêgo C, Garcia DG, Marques SA, Blanco Martinez
606 AM, Reis da Silva M, Marcondes de Souza J. Novel CCM1 (*KRIT1*)
607 Mutation Detection in Brazilian Familial Cerebral Cavernous
608 Malformation: Different Genetic Variants in Inflammation, Oxidative
609 Stress, and Drug Metabolism Genes Affect Disease Aggressiveness.
610 *World Neurosurg.* 2020;138:535-540.e8.
- 611 19. Choquet H, Pawlikowska L, Nelson J, McCulloch CE, Akers A, Baca B,
612 Khan Y, Hart B, Morrison L, Kim H. Polymorphisms in Inflammatory and
613 Immune Response Genes Associated with Cerebral Cavernous
614 Malformation Type 1 Severity. *Cerebrovasc. Dis.* [Internet]. 2014;38:433–
615 440. Available from: <https://www.karger.com/Article/FullText/369200>
- 616 20. Tang AT, Choi JP, Kotzin JJ, Yang Y, Hong CC, Hobson N, Girard R,
617 Zeineddine HA, Lightle R, Moore T, et al. Endothelial TLR4 and the

- 618 microbiome drive cerebral cavernous malformations. *Nature*.
619 2017;545:305–310.
- 620 21. Perrelli A, Retta SF. Polymorphisms in genes related to oxidative stress
621 and inflammation: Emerging links with the pathogenesis and severity of
622 Cerebral Cavernous Malformation disease. *Free Radic. Biol. Med.*
623 [Internet]. 2021;172:403–417. Available from:
624 <https://linkinghub.elsevier.com/retrieve/pii/S0891584921003865>
- 625 22. da Fontoura Galvão G, Fontes-Dantas FL, da Silva EV, Alves-Leon SV,
626 de Souza JM. Association of Variants in FCGR2A, PTPN2, and GM-CSF
627 with Cerebral Cavernous Malformation: Potential Biomarkers for a
628 Symptomatic Disease. *Curr. Neurovasc. Res.* [Internet]. 2021;18:172–
629 180. Available from: <https://www.eurekaselect.com/193838/article>
- 630 23. Lai CC, Nelsen B, Frias-Anaya E, Gallego-Gutierrez H, Orecchioni M,
631 Herrera V, Ortiz E, Sun H, Mesarwi OA, Ley K, et al. Neuroinflammation
632 Plays a Critical Role in Cerebral Cavernous Malformation Disease. *Circ.*
633 *Res.* [Internet]. 2022;131:909–925. Available from:
634 <https://www.ahajournals.org/doi/10.1161/CIRCRESAHA.122.321129>
- 635 24. McCole DF. Regulation of epithelial barrier function by the inflammatory
636 bowel disease candidate gene, PTPN2. *Ann. N. Y. Acad. Sci.* [Internet].
637 2012;1257:108–114. Available from:
638 <https://onlinelibrary.wiley.com/doi/10.1111/j.1749-6632.2012.06522.x>
- 639 25. Bottini N, Peterson EJ. Tyrosine Phosphatase PTPN22: Multifunctional
640 Regulator of Immune Signaling, Development, and Disease. *Annu. Rev.*
641 *Immunol.* [Internet]. 2014;32:83–119. Available from:
642 <https://www.annualreviews.org/doi/10.1146/annurev-immunol-032713-120249>
643
- 644 26. Santin I, Moore F, Colli ML, Gurzov EN, Marselli L, Marchetti P, Eizirik
645 DL. PTPN2 , a Candidate Gene for Type 1 Diabetes, Modulates
646 Pancreatic β -Cell Apoptosis via Regulation of the BH3-Only Protein Bim.
647 *Diabetes* [Internet]. 2011;60:3279–3288. Available from:
648 [https://diabetesjournals.org/diabetes/article/60/12/3279/14490/PTPN2-a-
649 Candidate-Gene-for-Type-1-Diabetes](https://diabetesjournals.org/diabetes/article/60/12/3279/14490/PTPN2-a-Candidate-Gene-for-Type-1-Diabetes)
- 650 27. Hsieh W-C, Svensson MN, Zoccheddu M, Tremblay ML, Sakaguchi S,
651 Stanford SM, Bottini N. PTPN2 links colonic and joint inflammation in
652 experimental autoimmune arthritis. *JCI Insight* [Internet]. 2020;5.
653 Available from: <https://insight.jci.org/articles/view/141868>
- 654 28. Shaw AM, Qasem A, Naser SA. Modulation of PTPN22 Function by
655 Spermidine in CRISPR-Cas9-Edited T-Cells Associated with Crohn's
656 Disease and Rheumatoid Arthritis. *Int. J. Mol. Sci.* [Internet].
657 2021;22:8883. Available from: [https://www.mdpi.com/1422-
658 0067/22/16/8883](https://www.mdpi.com/1422-0067/22/16/8883)
- 659 29. Ramagopalan S V, Heger A, Berlanga AJ, Maugeri NJ, Lincoln MR,
660 Burrell A, Handunnetthi L, Handel AE, Disanto G, Orton S-M, et al. A
661 ChIP-seq defined genome-wide map of vitamin D receptor binding:
662 Associations with disease and evolution. *Genome Res.* [Internet].
663 2010;20:1352–1360. Available from:
664 <http://genome.cshlp.org/lookup/doi/10.1101/gr.107920.110>

- 665 30. Ellis JA, Scurrah KJ, Li YR, Ponsonby A-L, Chavez RA, Pezic A, Dwyer T,
666 Akikusa JD, Allen RC, Becker ML, et al. Epistasis amongst PTPN2 and
667 genes of the vitamin D pathway contributes to risk of juvenile idiopathic
668 arthritis. *J. Steroid Biochem. Mol. Biol.* [Internet]. 2015;145:113–120.
669 Available from:
670 <https://linkinghub.elsevier.com/retrieve/pii/S0960076014002477>
- 671 31. Murray PJ. The primary mechanism of the IL-10-regulated
672 antiinflammatory response is to selectively inhibit transcription. *Proc. Natl.*
673 *Acad. Sci.* [Internet]. 2005;102:8686–8691. Available from:
674 <https://pnas.org/doi/full/10.1073/pnas.0500419102>
- 675 32. Sabat R, Grütz G, Warszawska K, Kirsch S, Witte E, Wolk K, Geginat J.
676 Biology of interleukin-10. *Cytokine Growth Factor Rev.* [Internet].
677 2010;21:331–344. Available from:
678 <https://linkinghub.elsevier.com/retrieve/pii/S1359610110000651>
- 679 33. Lyne SB, Girard R, Koskimäki J, Zeineddine HA, Zhang D, Cao Y, Li Y,
680 Stadnik A, Moore T, Lightle R, et al. Biomarkers of cavernous angioma
681 with symptomatic hemorrhage. *JCI Insight* [Internet]. 2019;4. Available
682 from: <https://insight.jci.org/articles/view/128577>
- 683 34. Mochol M, Taubøll E, Aukrust P, Ueland T, Andreassen OA, Svalheim S.
684 Interleukin 18 (IL-18) and its binding protein (IL-18BP) are increased in
685 patients with epilepsy suggesting low-grade systemic inflammation.
686 *Seizure* [Internet]. 2020;80:221–225. Available from:
687 <https://linkinghub.elsevier.com/retrieve/pii/S1059131120301473>
- 688 35. Gao F, Gao Y, Zhang S -j., Zhe X, Meng F-L, Qian H, Zhang B, Li Y-J.
689 Alteration of plasma cytokines in patients with active epilepsy. *Acta*
690 *Neurol. Scand.* [Internet]. 2017;135:663–669. Available from:
691 <https://onlinelibrary.wiley.com/doi/10.1111/ane.12665>
- 692 36. Girard R, Zeineddine HA, Fam MD, Mayampurath A, Cao Y, Shi C,
693 Shenkar R, Polster SP, Jesselson M, Duggan R, et al. Plasma
694 Biomarkers of Inflammation Reflect Seizures and Hemorrhagic Activity of
695 Cerebral Cavernous Malformations. *Transl. Stroke Res.* [Internet].
696 2018;9:34–43. Available from: [http://link.springer.com/10.1007/s12975-](http://link.springer.com/10.1007/s12975-017-0561-3)
697 [017-0561-3](http://link.springer.com/10.1007/s12975-017-0561-3)
- 698 37. Zhang C, Wang W, Zhang H, Wei L, Guo S. Association of FCGR2A
699 rs1801274 polymorphism with susceptibility to autoimmune diseases: A
700 meta-analysis. *Oncotarget.* 2016;7:39436–39443.
- 701 38. Duan J, Lou J, Zhang Q, Ke J, Qi Y, Shen N, Zhu B, Zhong R, Wang Z,
702 Liu L, et al. A genetic variant rs1801274 in FCGR2A as a potential risk
703 marker for Kawasaki disease: a case-control study and meta-analysis.
704 *PLoS One.* 2014;9:e103329.
- 705 39. Warmerdam PA, van de Winkel JG, Vlug A, Westerdaal NA, Capel PJ. A
706 single amino acid in the second Ig-like domain of the human Fc gamma
707 receptor II is critical for human IgG2 binding. *J. Immunol.* [Internet].
708 1991;147:1338–1343. Available from:
709 [https://journals.aai.org/jimmunol/article/147/4/1338/24700/A-single-amino-](https://journals.aai.org/jimmunol/article/147/4/1338/24700/A-single-amino-acid-in-the-second-Ig-like-domain)
710 [acid-in-the-second-Ig-like-domain](https://journals.aai.org/jimmunol/article/147/4/1338/24700/A-single-amino-acid-in-the-second-Ig-like-domain)
- 711 40. Shrestha S, Wiener HW, Olson AK, Edberg JC, Bowles NE, Patel H,

- 712 Portman MA. Functional FCGR2B gene variants influence intravenous
713 immunoglobulin response in patients with Kawasaki disease. *J. Allergy*
714 *Clin. Immunol.* [Internet]. 2011;128:677-680.e1. Available from:
715 <https://linkinghub.elsevier.com/retrieve/pii/S0091674911006646>
- 716 41. Hayat S, Babu G, Das A, Howlader ZH, Mahmud I, Islam Z. Fc-gamma
717 IIIa-V158F receptor polymorphism contributes to the severity of Guillain-
718 Barré syndrome. *Ann. Clin. Transl. Neurol.* 2020;7:1040–1049.
- 719 42. Mineo C, Gormley AK, Yuhanna IS, Osborne-Lawrence S, Gibson LL,
720 Hahner L, Shohet R V, Black S, Salmon JE, Samols D, et al. FcγRIIB
721 Mediates C-Reactive Protein Inhibition of Endothelial NO Synthase. *Circ.*
722 *Res.* [Internet]. 2005;97:1124–1131. Available from:
723 <https://www.ahajournals.org/doi/10.1161/01.RES.0000194323.77203.fe>
- 724 43. RYU J, LEE C, SHIN J, PARK C, KIM J, PARK S, HAN K. FcγRIIa
725 mediates C-reactive protein-induced inflammatory responses of human
726 vascular smooth muscle cells by activating NADPH oxidase 4.
727 *Cardiovasc. Res.* [Internet]. 2007;75:555–565. Available from:
728 <https://doi.org/10.1016/j.cardiores.2007.04.027>
- 729 44. Stein M-P, Edberg JC, Kimberly RP, Mangan EK, Bharadwaj D, Mold C,
730 Du Clos TW. C-reactive protein binding to FcγRIIa on human monocytes
731 and neutrophils is allele-specific. *J. Clin. Invest.* [Internet]. 2000;105:369–
732 376. Available from: <http://www.jci.org/articles/view/7817>
- 733 45. Raaz-Schrauder D, Ekici AB, Klinghammer L, Stumpf C, Achenbach S,
734 Herrmann M, Reis A, Garlich CD. The proinflammatory effect of C-
735 reactive protein on human endothelial cells depends on the FcγRIIa
736 genotype. *Thromb. Res.* [Internet]. 2014;133:426–432. Available from:
737 <https://linkinghub.elsevier.com/retrieve/pii/S0049384813006166>
- 738 46. Schneider MP, Leusen JHW, Herrmann M, Garlich CD, Amann K, John
739 S, Schmieder RE. The Fcγ receptor IIA R131H gene polymorphism is
740 associated with endothelial function in patients with
741 hypercholesterolaemia. *Atherosclerosis* [Internet]. 2011;218:411–415.
742 Available from:
743 <https://linkinghub.elsevier.com/retrieve/pii/S0021915011005880>
- 744 47. Gibson CC, Zhu W, Davis CT, Bowman-Kirigin JA, Chan AC, Ling J,
745 Walker AE, Goitre L, Delle Monache S, Retta SF, et al. Strategy for
746 Identifying Repurposed Drugs for the Treatment of Cerebral Cavernous
747 Malformation. *Circulation* [Internet]. 2015;131:289–299. Available from:
748 <https://www.ahajournals.org/doi/10.1161/CIRCULATIONAHA.114.010403>
- 749 48. Awad IA, Polster SP. Cavernous angiomas: deconstructing a
750 neurosurgical disease. *J. Neurosurg.* 2019;131:1–13.
- 751 49. Girard R, Khanna O, Shenkar R, Zhang L, Wu M, Jesselson M,
752 Zeineddine HA, Gangal A, Fam MD, Gibson CC, et al. Peripheral plasma
753 vitamin D and non-HDL cholesterol reflect the severity of cerebral
754 cavernous malformation disease. *Biomark. Med.* 2016;10:255–264.
- 755 50. Akers A, Al-Shahi Salman R, A. Awad I, Dahlem K, Flemming K, Hart B,
756 Kim H, Jusue-Torres I, Kondziolka D, Lee C, et al. Synopsis of Guidelines
757 for the Clinical Management of Cerebral Cavernous Malformations:
758 Consensus Recommendations Based on Systematic Literature Review by

- 759 the Angioma Alliance Scientific Advisory Board Clinical Experts Panel.
760 *Neurosurgery* [Internet]. 2017;80:665–680. Available from:
761 <https://journals.lww.com/00006123-201705000-00012>
- 762 51. Krasniqi E, Boshnjaku A, Wagner K-H, Wessner B. Association between
763 Polymorphisms in Vitamin D Pathway-Related Genes, Vitamin D Status,
764 Muscle Mass and Function: A Systematic Review. *Nutrients* [Internet].
765 2021;13:3109. Available from: [https://www.mdpi.com/2072-](https://www.mdpi.com/2072-6643/13/9/3109)
766 [6643/13/9/3109](https://www.mdpi.com/2072-6643/13/9/3109)
- 767 52. Uitterlinden AG, Fang Y, van Meurs JBJ, Pols HAP, van Leeuwen JPTM.
768 Genetics and biology of vitamin D receptor polymorphisms. *Gene*
769 [Internet]. 2004;338:143–156. Available from:
770 <https://linkinghub.elsevier.com/retrieve/pii/S0378111904003075>
- 771 53. Jiang P, Zhu W-Y, He X, Tang M-M, Dang R-L, Li H-D, Xue Y, Zhang L-
772 H, Wu Y-Q, Cao L-J. Association between Vitamin D Receptor Gene
773 Polymorphisms with Childhood Temporal Lobe Epilepsy. *Int. J. Environ.*
774 *Res. Public Health* [Internet]. 2015;12:13913–13922. Available from:
775 <http://www.mdpi.com/1660-4601/12/11/13913>
- 776 54. Fouad H, Yahia S, Elsaid A, Hammad A, Wahba Y, El-Gilany A-H, Abdel-
777 Aziz A-AF. Oxidative stress and vitamin D receptor Bsm1 gene
778 polymorphism in Egyptian children with systemic lupus erythematosus: a
779 single center study. *Lupus*. 2019;28:771–777.
- 780 55. Ghaly MS, Badra DI, Dessouki O, Elmaraghy NN, Hassan R. Vitamin D
781 receptor Fok1 & Bsm 1 Gene Polymorphisms in Systemic Lupus
782 Erythematosus and Osteoarthritis: Autoimmune Inflammatory versus
783 Degenerative Model. *Egypt. J. Immunol.* 2017;24:151–164.
- 784 56. Tizaoui K, Hamzaoui K. Association between VDR polymorphisms and
785 rheumatoid arthritis disease: Systematic review and updated meta-
786 analysis of case-control studies. *Immunobiology*. 2015;220:807–816.
- 787 57. Stockton RA, Shenkar R, Awad IA, Ginsberg MH. Cerebral cavernous
788 malformations proteins inhibit Rho kinase to stabilize vascular integrity. *J.*
789 *Exp. Med.* 2010;207:881–896.
- 790 58. Borikova AL, Dibble CF, Sciaky N, Welch CM, Abell AN, Bencharit S,
791 Johnson GL. Rho kinase inhibition rescues the endothelial cell cerebral
792 cavernous malformation phenotype. *J. Biol. Chem.* 2010;285:11760–
793 11764.
- 794 59. Whitehead KJ, Chan AC, Navankasattusas S, Koh W, London NR, Ling J,
795 Mayo AH, Drakos SG, Jones CA, Zhu W, et al. The cerebral cavernous
796 malformation signaling pathway promotes vascular integrity via Rho
797 GTPases. *Nat. Med.* 2009;15:177–184.
- 798 60. Crose LES, Hilder TL, Sciaky N, Johnson GL. Cerebral cavernous
799 malformation 2 protein promotes smad ubiquitin regulatory factor 1-
800 mediated RhoA degradation in endothelial cells. *J. Biol. Chem.*
801 2009;284:13301–13305.
- 802 61. Morelli A, Vignozzi L, Filippi S, Vannelli GB, Ambrosini S, Mancina R,
803 Crescioli C, Donati S, Fibbi B, Colli E, et al. BXL-628, a vitamin D receptor
804 agonist effective in benign prostatic hyperplasia treatment, prevents
805 RhoA activation and inhibits RhoA/Rho kinase signaling in rat and human

- 806 bladder. *Prostate*. 2007;67:234–247.
- 807 62. Amur S, LaVange L, Zineh I, Buckman-Garner S, Woodcock J. Biomarker
808 Qualification: Toward a Multiple Stakeholder Framework for Biomarker
809 Development, Regulatory Acceptance, and Utilization. *Clin. Pharmacol.*
810 *Ther.* [Internet]. 2015;98:34–46. Available from:
811 <https://onlinelibrary.wiley.com/doi/10.1002/cpt.136>
- 812 63. von Elm E, Altman DG, Egger M, Pocock SJ, Gøtzsche PC,
813 Vandembroucke JP. The Strengthening the Reporting of Observational
814 Studies in Epidemiology (STROBE) statement: guidelines for reporting
815 observational studies. *Lancet* [Internet]. 2007;370:1453–1457. Available
816 from: <https://linkinghub.elsevier.com/retrieve/pii/S014067360761602X>
- 817 64. Fontes FL, de Araújo LF, Coutinho LG, Leib SL, Agnez-Lima LF. Genetic
818 polymorphisms associated with the inflammatory response in bacterial
819 meningitis. *BMC Med. Genet.* [Internet]. 2015;16:1–12. Available from:
820 <http://dx.doi.org/10.1186/s12881-015-0218-6>
- 821 65. Chehuen Bicalho V, da Fontoura Galvão G, Lima Fontes-Dantas F, Paulo
822 da Costa Gonçalves J, Dutra de Araujo A, Carolina França L, Emílio
823 Corrêa Leite P, Campolina Vidal D, Castro Filho R, Vieira Alves-Leon S,
824 et al. Asymptomatic cerebral cavernous angiomas associated with plasma
825 marker signature. *J. Clin. Neurosci.* [Internet]. 2021;89:258–263.
826 Available from:
827 <https://linkinghub.elsevier.com/retrieve/pii/S0967586821001910>
- 828 66. da Fontoura Galvão G, da Silva EV, Trefilio LM, Alves-Leon SV, Fontes-
829 Dantas FL, de Souza JM. Comprehensive CCM3 Mutational Analysis in
830 Two Patients with Syndromic Cerebral Cavernous Malformation. *Transl.*
831 *Stroke Res.* [Internet]. 2023; Available from:
832 <https://link.springer.com/10.1007/s12975-023-01131-x>
- 833 67. Pettersen EF, Goddard TD, Huang CC, Couch GS, Greenblatt DM, Meng
834 EC, Ferrin TE. UCSF Chimera?A visualization system for exploratory
835 research and analysis. *J. Comput. Chem.* [Internet]. 2004;25:1605–1612.
836 Available from: <https://onlinelibrary.wiley.com/doi/10.1002/jcc.20084>
- 837 68. Edgar RC. MUSCLE: multiple sequence alignment with high accuracy
838 and high throughput. *Nucleic Acids Res.* [Internet]. 2004;32:1792–1797.
839 Available from: [https://academic.oup.com/nar/article-](https://academic.oup.com/nar/article-lookup/doi/10.1093/nar/gkh340)
840 [lookup/doi/10.1093/nar/gkh340](https://academic.oup.com/nar/article-lookup/doi/10.1093/nar/gkh340)

841

842

843

844

845 **Legend Figures**

846

847 Figure 1: Association of *PTPN2* and *VDR* to a Symptomatic Phenotype, Linkage
848 Disequilibrium Map and Plasmatic Cytokine Expression. (A) Haplotype map
849 showing the 3 SNPs analyzed and the range of R^2 value, suggesting that
850 $VDR^{rs7975232}$ and $VDR^{rs731236}$ are in linkage disequilibrium ($D' > 0.99$), while the

851 other combinations segregate independently $VDR^{rs11568820}$ and $VDR^{rs731236}$
852 ($D' > 0.04$), $VDR^{rs11568820}$ and $VDR^{rs7975232}$ ($D' > 0.317$). (B) ROC analysis
853 evidencing the performance of $PTPN2^{rs72872125}$ CT genotype (AUC 0.420) and (C)
854 $VDR^{rs7975232}$ CC (AUC 0.439) to distinguish symptomatic patients. (D) Plasmatic
855 cytokine expression between $PTPN2^{rs72872125}$ groups showing the $PTPN2^{rs72872125}$
856 CT genotype have higher plasma level of IL-10 ($p = 0.0146$), (E) low levels of IL-
857 18 ($p = 0.0450$) and (F) low levels of IFN- γ ($p = 0.0310$) (Figure 1F), while
858 individuals with at least one $VDR^{rs7975232}$ C allele had (G) low plasma levels of IL-
859 27 ($p = 0.0055$) and (H) low plasma levels of IL-23 ($p = 0.0034$).

860

861 Figure 2: *Performance of Diagnostic Biomarker*. (A) ROC curve of the best
862 weighted-biomarker included $PTPN2^{rs72872125}$ CC genotype and GMCSF plasma
863 levels as formulated $-0,89*(GMCSF)+0,41*(PTPN2^{rs72872125}CC)$ (AUC 0.663, SE
864 0.06 CI 95% 0.534 – 0.792, $p = 0.01$) with a specificity and sensitivity 85.7% and
865 41.3%, respectively. (B) The median weighted combination value was 2.65-times
866 increased ($p = 0.01$) in symptomatic patients (median estimated value -0.36)
867 compared with asymptomatic individuals (median estimated value -0.97). Sub-
868 group analysis demonstrating that the formula performed fairly in the sub-group
869 analysis of (C) symptomatic bleeding patients (AUC 0.661, SE 0.07, CI 95%
870 0.517 – 0.806) but had a good accuracy in (D) familiar form of the disease (AUC
871 0.774, SE 0.09, CI 95% 0.595 – 0.953, $p = 0.01$) and (E) patients with
872 infratentorial lesions (AUC 0.804, SE 0.08, CI 95% 0.642 – 0.966, $p = 0.001$).

873

874 Figure 3: *Performance of Prognostic Biomarker and In Silico Structural Analysis*
875 *of Transcript FCGR2A^{rs180127}*. (A) The weighted-biomarker had a fair accuracy
876 (AUC 0.644, SE 0.078, CI 95% 0.491-0.976) as prognostic biomarker while
877 $FCGR2A^{rs1801274}$ GG (B) genotype had an excellent accuracy (AUC 0.796, SE
878 0.12, CI 95% 0.631-0.897) in distinguishing these patients. (C) ROC curve
879 evidencing the performance of the $FCGR2A^{rs1801274}$ GG genotype after PSM
880 analysis (AUC 0.875) and (D) in a sub-group of pure asymptomatic patients (AUC
881 0.829). (E) *In silico* structural analysis prediction reveals that the $FCGR2A^{rs1801274}$
882 leads to a substitution of a histidine for an arginine at position 131 leading to a
883 predicted conformational structure slightly different than the wild-type. (F)

884 Structural alignment predicts that the mutation c.500A>G (p.His131Arg) occurred
885 in domain conserved in higher primates, within 30% of the species sharing this site.

886

887 Figure 4: *Kaplan-Meier curve demonstrating that VDR variants are related to*
888 *Precocity of symptoms.* (A) $VDR^{rs731236}$ AA genotype tend to have symptoms later
889 in life compared to those who did not have (HR 0.52, $p = 0.020$). (B) Individuals
890 that harbor the $VDR^{rs11568820}$ CC genotype tend to have symptoms earlier (HR
891 1.58, $p = 0.016$).

892

893 **TABLES**

894

895 Table 1: Studied SNPs and their basic characteristics and female sex adjusted
896 multivariable analysis.

Gene	SNP ID	Alternative Name	Chr/Location	Nucleotide Change	Aminoacid Change	MAF ALFA
<i>PTPN2</i>	rs72872125		18/intron	C>T		0.11
<i>VDR</i>	rs7975232	Apa1	12/intron	C>A		0.55
	rs731236	Taq1	12/exon	A>G	Ile > Ile	0.38
	rs11568820		12/intron	C>T		0.28
<i>FCGR2A</i>	rs1801274		1/exon	A>G	His > Arg	0.51

897

898 Chr - chromosome; MAF - minimal allele frequency

899

900 Table 2: Summary of the Demographic and Clinical Characteristics

Characteristics	N (%)	Multifocal/Familiar	Age (years), mean	Sex: Female, n
Asymptomatic	33 (32%)	13	46.3	22
Symptomatic	70 (67%)	31	45.3	43
Hemorrhage	48 (46%)	20	41.6	33
Epilepsy	22 (21%)	11	53.7	10
Total	103	44	45.6	65

901

902 N - absolute number

903

904

905

906 Table 3: Association between SNPs and Different Phenotypes in the age,
907 familiar and female sex adjusted multivariable analysis

Gene	SNP ID	Allele	Symptomatic	Asymptomatic	OR (95% CI)	<i>P</i>
<i>PTPN2</i>	rs72872125	CC	59	22	2.83 (1.04-7.67)	0.04
		CT	8	9	0.34 (0.11-0.99)	
<i>VDR</i>	rs7975232	CC	1	5	0.06 (0.006-0.6120)	0.017
		AC	20	5	2.33 (0.782-6.949)	0.128
		AA	47	22	1.00 (0.403-2.500)	0.993
	rs731236	GG	12	3	2.16 (0.525 - 8.942)	0.779
		AG	21	16	1.06 (0.408-2.789)	0.893
		AA	30	14	0.89 (0.349-2.220)	0.808
	rs11568820	TT	15	5	1.36 (0.434 - 4.298)	0.893
		CT	25	14	0.73 (0.298-1.817)	0.507
		CC	30	12	0.71 (0.288-1.783)	0.474
<i>FCGR2A</i>	rs1801274	GG	19	8	1.14 (0.438 - 3.007)	0.962
		AG	36	14	0.71 (0.288-1.771)	0.469
		AA	14	11	0.71 (0.288-1.775)	0.471

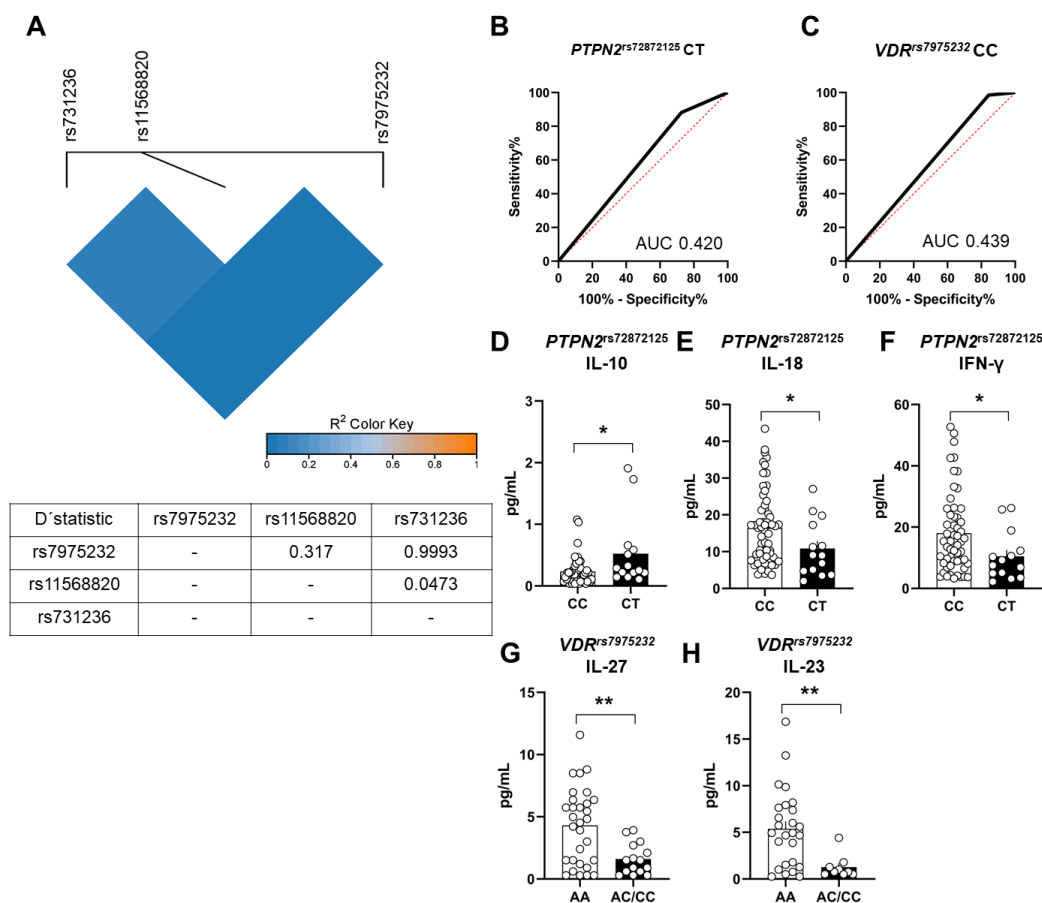
908

909 *OR: Odds Ratio; CI: Confidential Interval. Data analyzed through binary logistic*
910 *regression. P < 0.05 are highlighted in bold*

911

912

913 **Figure 1**



914

915

916

917

918

919

920

921

922

923

924

925

926

927

928

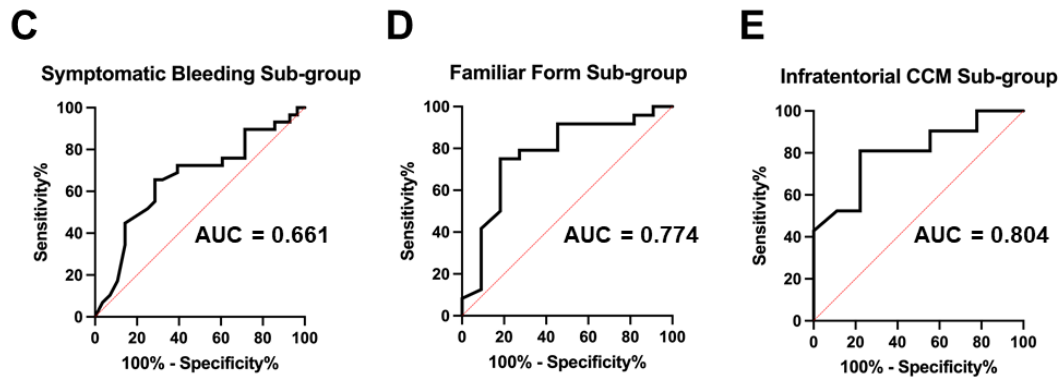
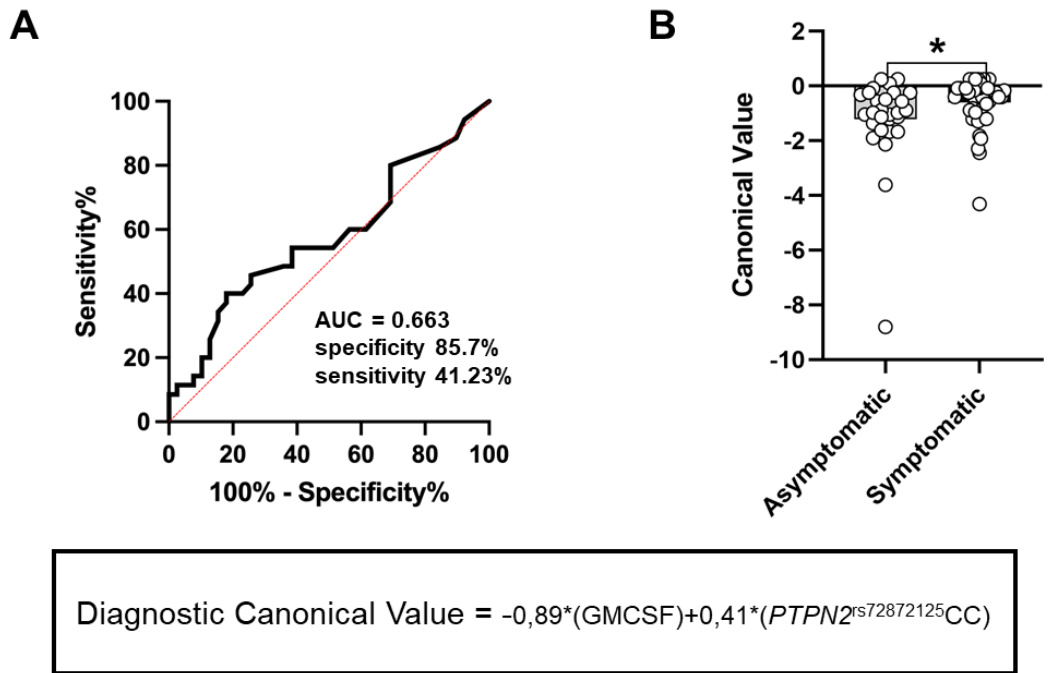
929

930

931

932

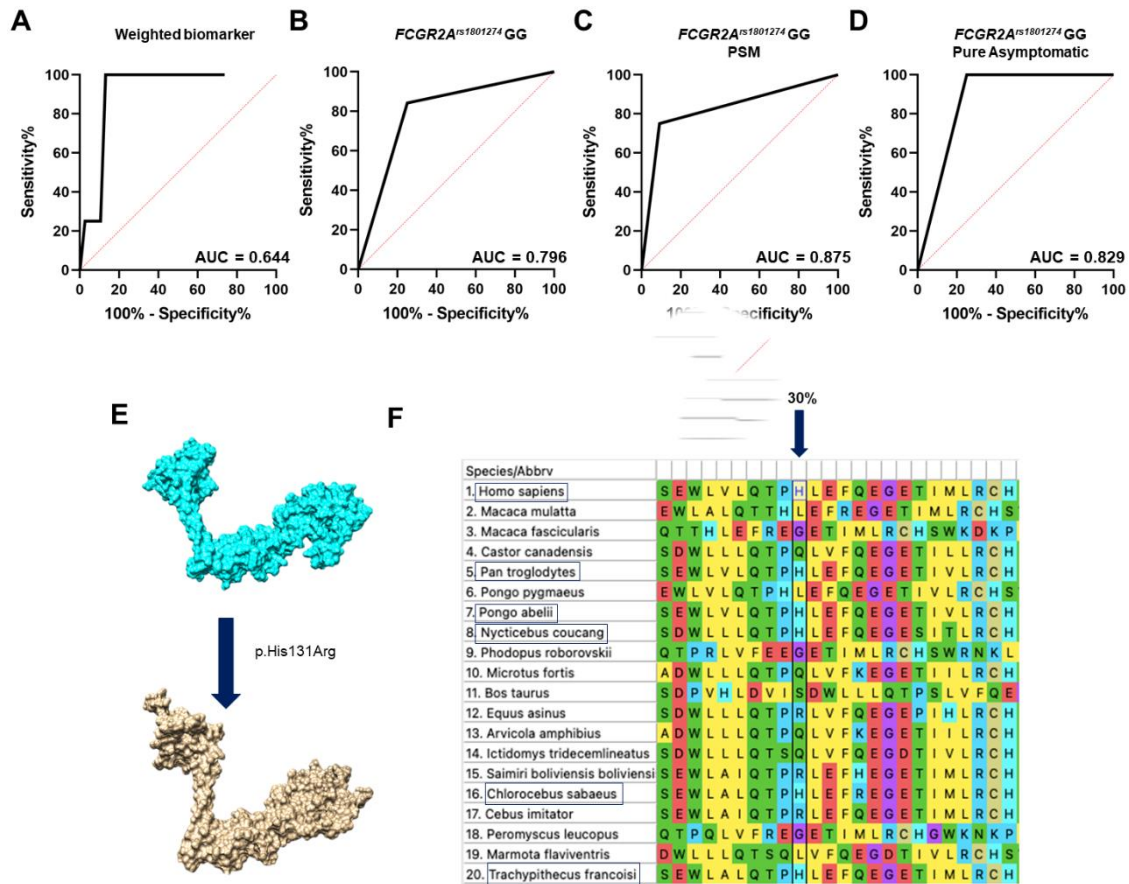
933 **Figure 2**



934
935
936
937
938
939
940
941
942
943
944
945
946
947
948

949 **Figure 3**

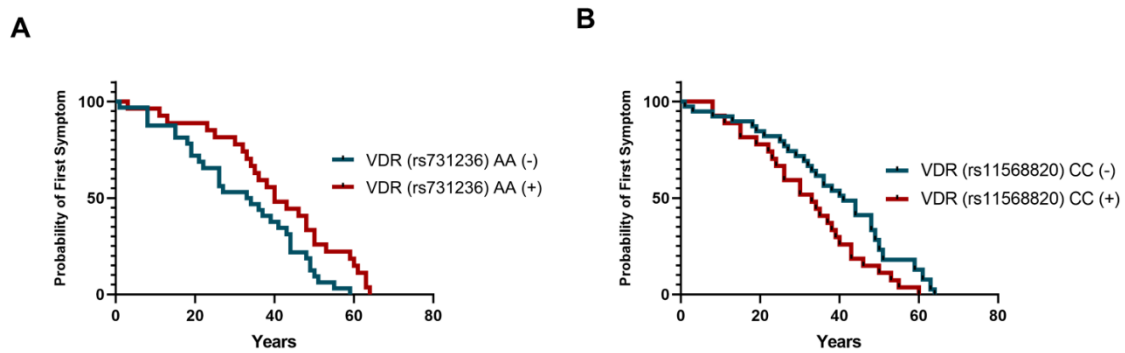
950



951

952

953 **Figure 4**



954

955

956

957